ORIGINAL RESEARCH ARTICLE

Soil hydraulic properties estimation from one-dimensional infiltration experiments using characteristic time concept

Mehdi Rahmati[1,2] | Jan Vanderborght[2] | Jirka Šimůnek[3] | Jasper A. Vrugt[4,5] |
David Moret-Fernández[6] | Borja Latorre[6] | Laurent Lassabatere[7] |
Harry Vereecken[2]

[1] Dep. of Soil Science and Engineering, Faculty of Agriculture, Univ. of Maragheh, Maragheh, Iran

[2] Institute of Bio- and Geosciences: Agrosphere (IBG-3), Forschungszentrum Jülich, Jülich, Germany

[3] Dep. of Environmental Sciences, Univ. of California, Riverside, CA 92507, USA

[4] Dep. of Civil and Environmental Engineering, Univ. of California, Irvine, CA 92697, USA

[5] Dep. of Earth System Science, Univ. of California, Irvine, CA 92697, USA

[6] Dep. de Suelo y Agua, Estación Experimental de Aula Dei, Consejo Superior de Investigaciones Científicas (CSIC), PO Box 13034, Zaragoza 50080, Spain

[7] Univ. Lyon, Univ. Claude Bernard Lyon 1, CNRS, ENTPE, UMR5023 LEHNA, Vaulx-en-Velin F-69518, France

Correspondence
Mehdi Rahmati, Dep. of Soil Science and Engineering, Faculty of Agriculture, Univ. of Maragheh, Maragheh, Iran; Institute of Bio- and Geosciences: Agrosphere (IBG-3), Forschungszentrum Jülich, Jülich, Germany.
Email: mehdirmti@gmail.com.
Harry Vereecken, Institute of Bio- and Geosciences: Agrosphere (IBG-3), Forschungszentrum Jülich, Jülich, Germany.
Email: h.vereecken@fz-juelich.de

Abstract

Many different equations ranging from simple empirical to semi-analytical solutions of the Richards equation have been proposed for quantitative description of water infiltration into variably saturated soils. The sorptivity, S, and the saturated hydraulic conductivity, K_s, in these equations are typically unknown and have to be estimated from measured data. In this paper, we use so-called characteristic time (t_{char}) to design a new method, referred to as the characteristic time method (CTM) that estimates S, and K_s, from one-dimensional (1D) cumulative infiltration data. We demonstrate the usefulness and power of the CTM by comparing it with a suite of existing methods using synthetic cumulative infiltration data simulated by HYDRUS-1D for 12 synthetic soils reflecting different USDA textural classes, as well as experimental data selected from the Soil Water Infiltration Global (SWIG) database. Results demonstrate that the inferred values of S and K_s are in excellent agreement with their theoretical values used in the synthetically simulated infiltration experiments with Nash–Sutcliffe criterion close to unity and RMSE values of 0.04 cm h$^{-1/2}$ and 0.05 cm h^{-1}, respectively. The CTM also showed very high accuracy when applied on synthetic data with added measurement noise, as well as robustness when applied to experimental data. Unlike previously published methods, the CTM does not require knowledge of the time

Abbreviations: CF2, two-term curve-fitting model; CF3, three-term curve-fitting model; CTM, characteristic time method; 1D, one-dimensional; QEI, quasi-exact implicit; SH, Sharma; SWIG, Soil Water Infiltration Global; VGM, van Genuchten–Mualem.

validity of the applied semi-analytical solution for infiltration and, therefore, is applicable to infiltrations with durations from 5 min to several days. A script written in Python of the CTM method is provided in the supplemental material.

1 | INTRODUCTION

Accurate and reliable estimation of hydraulic properties of variably saturated soils from infiltration experiments is still a major challenge in many research fields such as hydrology, irrigation, civil engineering, and environmental science (Moret-Fernández, Latorre, & Angulo-Martínez, 2017; Valiantzas, 2010). In the past decades, a large number of theoretical, semiempirical, and empirical models have appeared in the literature that quantitatively describe water infiltration into the soil (Green & Ampt, 1911; Haverkamp, Ross, Smettem, & Parlange, 1994; Parlange, Lisle, Braddock, & Smith, 1982; Philip, 1957; Swartzendruber, 1987). These models were used for the characterization of soil hydraulic properties, including soil sorptivity (S) and saturated hydraulic conductivity (K_s). According to their theoretical definitions, S is a measurable physical quantity, which expresses the capacity of a porous medium to take up and release liquids by capillarity (Philip, 1957), whereas K_s measures the soil's ability to transmit water under the influence of gravity.

In general, there are two major approaches to estimate S and K_s from one-dimensional (1D) infiltration experiments considered in the literature: (a) linearization approaches and (b) inverse estimation of S and K_s using curve-fitting methods. Table 1 summarizes the most often used linearization methods to predict S and K_s from 1D infiltration curves using Philip's (1957) two-term equation ($I = St^{1/2} + cK_st$, where t represents time and c is a constant).

The linearity of the linearized model proposed by Smiles and Knight (1976) for long-time intervals indicates an appropriate description of the infiltration process by the two-term equation and that values of S and K_s can be determined from the y intercept and the slope of the line, respectively. However, there is still substantial arbitrariness in deciding when the linear part stops and nonlinearity starts, and in detection of a plausibly linear relationship, leading

to uncertainty in estimated values depending on the choice made.

The linearization method proposed by Sharma, Gander, and Hunt (1980) is motivated by the fact that capillary forces, and thus S, dominate the infiltration process at early stages, whereas at later stages, the impact of capillary forces decreases and the gravitational force becomes dominant. Therefore, they proposed to determine S from infiltration measurements at early time steps where one can assume a linear relationship between I and $\sqrt{t}$ in Philip's two-term equation by setting K_s to zero. They also indicated that the $I(t)$ vs. t plot usually shows a linear relationship for long times when infiltration reaches steady-state conditions. However, if the duration of infiltration measurements is not long enough to reach such a steady-state condition, this method will, in most cases, overestimate K_s. They also indicated that the slope of the $I(t)$ vs. t plot is equal to K_s at the end. In fact, for short times (transient state), the slope is approximately equal to $(2 - \beta)/3 \times K_s$ (where $\beta = 0.6$; Haverkamp et al., 1994). When we get closer to the steady state, the value of the slope tends towards K_s. On the other hand, the steady-state infiltration corresponds to an intercept + $K_s \times t$ that may not be negligible. This is especially the case for fine-textured soils where the intercept, which is related to the ratio between S^2 and K_s (Haverkamp et al., 1994), takes large values.

We do not discuss the differentiated linearization method of Vandervaere, Vauclin, and Elrick (2000), and it is excluded from further comparisons. Indeed, Angulo-Jaramillo et al. (2000) found that this method is only applicable for short to medium times, and its validity may be questionable when a steady state is reached too quickly. Latorre, Peña, Lassabatere, Angulo-Jaramillo, and Moret-Fernández (2015) also used this method to determine S and K_s from infiltration measurements using a disk infiltrometer and demonstrated that it is inaccurate to derive soil hydraulic parameters. On the other hand, the

TABLE 1 Most often used linearization methods to predict soil sorptivity (S) and saturated hydraulic conductivity (K_s) from one-dimensional infiltration curves using Philip's (1957) two-term equation ($I = St^{1/2} + cK_st$)

Procedure	Linearized model	Proposed by
Cumulative linearization	$It^{-1/2} = S + cK_st^{1/2}$	Smiles and Knight (1976)
Two-part linearization	$I = St^{1/2}$ for early times; $I = K_st$ for later times	Sharma et al. (1980)
Differentiated linearization	$\Delta I(t)/\Delta\sqrt{t} = S + 2A_2(\sqrt{t_it_{i+1}})^{\frac{1}{2}}$	Vandervaere et al. (2000)

Note. I, infiltration; t, time; c and A_2, infiltration constants; i, subscript ranging from 1 to the number of data points in the infiltration curve.

Vandervaere et al. (2000) method was mainly intended for disc infiltrometer measurements, where a contact sand layer is placed between the soil surface and the base disc. According to Moret-Fernández, Blanco, Martínez-Chueca, and Bielsa (2013), without a contact sand layer, the Smiles and Knight (1976) method performs much better than the Vandervaere et al. (2000) one. Therefore, since we are working with 1D infiltration curves generated without using a contact sand layer, it was rational to exclude this method from further analysis.

The second major approach uses curve fitting (Bonell & Williams, 1986; Bristow & Savage, 1987; Marquardt, 1963; Vandervaere et al., 2000) of nonlinear infiltration equations in time to estimate soil hydraulic properties. Typically, an objective function that involves squared differences between measured and predicted infiltration rates or cumulative infiltration volumes is minimized by changing S and K_s. Philip's (1957) two-term equation, due to its simplicity, is usually used with the curve fitting method to determine S and K_s. However, Vandervaere et al. (2000) pointed out that although the determination of hydraulic properties (S and K_s) using Philip's two-term equation is a well-posed problem, since it has only two degrees of freedom for scale and shape, the obvious correlation between $\sqrt{t}$ and t makes it a relatively ill-conditioned problem where an increase in one parameter can be compensated by a decrease in the other parameter. Additionally, the curve fitting of Philip's two-term equation only provides physically consistent parameters if the time validity domain of the equation is considered.

Although the curve-fitting procedure usually results in a very good agreement ($R^2 > .9$) between measured and predicted infiltration curves, the predicted parameters may be far from their true values. Equifinality, the principle that the minimum of the objective function can be obtained by a broad set of parameter values (Beven & Freer, 2001), is the main reason why no one can guarantee the results obtained using the curve-fitting method. Vandervaere et al. (2000) criticized this method by simply stating that "the best fit does not necessarily mean good fit."

In order to overcome the arbitrariness of the linearization method and equifinality of the curve-fitting method, we present a new procedure based on the use of the characteristic time to uniquely predict S and K_s from infiltration experiments while implicitly accounting for the time domain validity. Therefore, we use in our proposed method (hereafter called the characteristic time method [CTM]) the gravity time, t_{grav}, defined as the time when gravity and capillarity have exactly the same impact on infiltration, to predict S and K_s. In a similar manner, t_{grav} was also used to give an idea about the transition time that separates the steady from the transient regimes of water infiltration (Lassabatere et al., 2006; Philip, 1969b). We test the proce-

Core Ideas

- A new method named CTM is proposed to estimate the S and K_s from 1D infiltration curve.
- The CTM takes the advantages of the characteristic time in prediction of S and K_s.
- The CTM was more accurate than the nonlinear curve fitting method in simultaneous prediction of S and K_s.
- The CTM was applicable to any infiltration duration of 15 min to several days.

dure against the curve-fitting method using two- (CF2) or three-term (CF3) models and the method of Sharma et al. (1980) (SH). The CTM and SH methods that we compare are not limited in time because they both treat the data over the entire course of the infiltration (including transient and steady states).

2 | THEORETICAL BACKGROUND

2.1 | New procedure development

In order to characterize the 1D infiltration process, Philip (1957) derived a semianalytical solution of the Richards (1931) equation for ponded infiltration in unsaturated soils for the transient state. Philip's time series expansion for cumulative infiltration can be written as

$$I(t) = A_1 t^{0.5} + A_2 t + A_3 t^{\frac{3}{2}} + A_4 t^2 + A_5 t^{\frac{5}{2}}$$
$$+ \sum_{i=6}^{n} A_i t^{\frac{i}{2}} \tag{1}$$

where I [L] denotes the cumulative infiltration, t [T] signifies time, A_1 [L T$^{-1/2}$] to A_5 [L T$^{-1/2}$] are coefficients, and

$$\sum_{i=6}^{n} A_i t^{\frac{i}{2}}$$

represent higher order terms that are much smaller than the lower orders and can therefore be neglected. Philip (1957) showed that A_1 is equal to the sorptivity S [L T$^{-1/2}$], A_2 [L T^{-1}] is proportional to the saturated hydraulic conductivity K_s [L T^{-1}], and the coefficients with $n > 2$ must satisfy

$$\frac{A_n}{S} > \left(\frac{A_2}{S} \right)^{n-1} \tag{2}$$

It is important to note that Equation 1 remains valid over the time interval $[0, t_{\max}]$, where $t_{\max}$ increases with n. Accounting for more orders allows the extension of the time validity interval. However, in all cases, the expansions must be restricted to the given validity time intervals and thus address the case of transient state. Philip (1957) introduced the gravity time, t_{grav} [T], for the identification of the validity time for the case of the two-term expansion.

To remedy problems with the time validity of infiltration models, Haverkamp et al. (1994) derived a quasi-exact implicit (QEI) solution of the Richards equation to describe 1D cumulative infiltration, which was firstly proposed by Parlange et al. (1982) and then redefined by Haverkamp, Parlange, Starr, Schmitz, and Fuentes (1990):

$$
\frac{2(K_{\mathrm{s}}-K_{\mathrm{i}})^2}{S^2}t = \frac{2}{1-\beta}\frac{(K_{\mathrm{s}}-K_{\mathrm{i}})[I(t)-K_{\mathrm{i}}t]}{S^2} - \frac{1}{1-\beta}
$$
$$
\ln\left(\frac{1}{\beta}\exp\left\{\frac{2\beta(K_{\mathrm{s}}-K_{\mathrm{i}})[I(t)-K_{\mathrm{i}}t]}{S^2}\right\} + \frac{\beta-1}{\beta}\right) \tag{3}
$$

where K_{i} and K_{s} are soil hydraulic conductivities at initial and saturated water contents of θ_{i} and θ_{s}, respectively, and β (dimensionless) is an integral infiltration constant that is either fixed at 0.6 or that can be computed soil specifically as follows (Haverkamp et al., 1994):

$$
\beta = 2 - 2\frac{\int_{\theta_{\mathrm{i}}}^{\theta_{\mathrm{s}}}\left(\frac{K(\theta)-K_{\mathrm{i}}}{K_{\mathrm{s}}-K_{\mathrm{i}}}\right)\left(\frac{\theta_{\mathrm{s}}-\theta_{\mathrm{i}}}{\theta-\theta_{\mathrm{i}}}\right)D(\theta)\mathrm{d}\theta}{\int_{\theta_{\mathrm{i}}}^{\theta_{\mathrm{s}}}D(\theta)\mathrm{d}\theta} \tag{4}
$$

where $K(\theta)$ and $D(\theta)$ are hydraulic conductivity and diffusivty, respectively, of soil water at a given soil water content of θ.

Haverkamp et al. (1994) proposed an approximate time expansion of Equation 3 for the description of the transient state considering a two-term equation in line with Philip (1957) two-term equation:

$$
I(t) = c(1)t^{0.5} + c(2)t \tag{5}
$$

where

$$
\begin{aligned}
c(1) &= S \\
c(2) &= \frac{2-\beta}{3}K_{\mathrm{s}}
\end{aligned} \tag{6}
$$

As stated above, the Equation 5 is valid for short to intermediate times only. Recently, Rahmati, Latorre, Lassabatere, Angulo-Jaramillo, and Moret-Fernández (2019) provided the three-term expansion of the QEI solution of Haverkamp et al. (1994), which is valid for longer times compared with Equation 5 and is identical to the Philip (1957) three-term equation:

$$
I(t) = c(1)t^{0.5} + c(2)t + c(3)t^{3/2} \tag{7}
$$

where $c(1)$ and $c(2)$ are as previously defined, and $c(3)$ is

$$
c(3) = \frac{1}{9}\left(\beta^2 - \beta + 1\right)\frac{K_{\mathrm{s}}^2}{S} \tag{8}
$$

Similarly to Rahmati et al. (2019), one can apply the Taylor series expansion (in powers of 0.5) to the QEI formulation to introduce the fifth (or any other) term of the approximate expansion. The following equation presents the approximate expansion up to the fifth term:

$$
\begin{aligned}
I(t) &= c(1)t^{1/2} + c(2)t + c(3)t^{3/2} \\
&+ c(4)t^2 + c(5)t^{5/2}
\end{aligned} \tag{9}
$$

where $c(1)$ to $c(3)$ are defined as before, and $c(4)$ and $c(5)$ are defined as

$$
\begin{aligned}
c(4) &= \frac{2}{135}(\beta - 2)(\beta + 1)(1 - 2\beta)\frac{K_{\mathrm{s}}^3}{S^2} \\
c(5) &= \frac{1}{270}\left(\beta^2 - \beta + 1\right)^2\frac{K_{\mathrm{s}}^4}{S^3}
\end{aligned} \tag{10}
$$

If we divide both the right and left sides of Equation 9 by $I(t)$, we get the following equation depicting the contribution (W) of each term to the infiltration process:

$$
W_i = \frac{c(i)t^{i/2}}{I(t)}, i = 1, 2, \ldots, 5 \tag{11}
$$

where

$$
W_1 + W_2 + W_3 + W_4 + W_5 = 1 \tag{12}
$$

In Equation 12, we assume that the contribution of the higher order terms (orders > 5) are negligible and that we remain in the validity time interval related to the five-term approximate expansion. By plotting the contributions of different components to a simulated infiltration curve for known values of S and K_{s} (Figure 1), we can outline the following facts:

I. At the start of the infiltration process ($t = 0$), the contribution of the first term to the infiltration process is maximal and equal to one, whereas the integrated contribution of remaining terms is equal to zero (Figures 1b and 1c).

II. At a time equal to t_{grav}, the contribution of the first term is equal to the integrated contribution of the remaining terms, both being equal to 0.5 (Figure 1c).

III. Similar to second term, the third and subsequent terms act as gravity components since they have zero contributions on infiltration at initial time steps and nonzero contribution at later time steps (Figure 1b) where the contributions are increased by advancing in time.
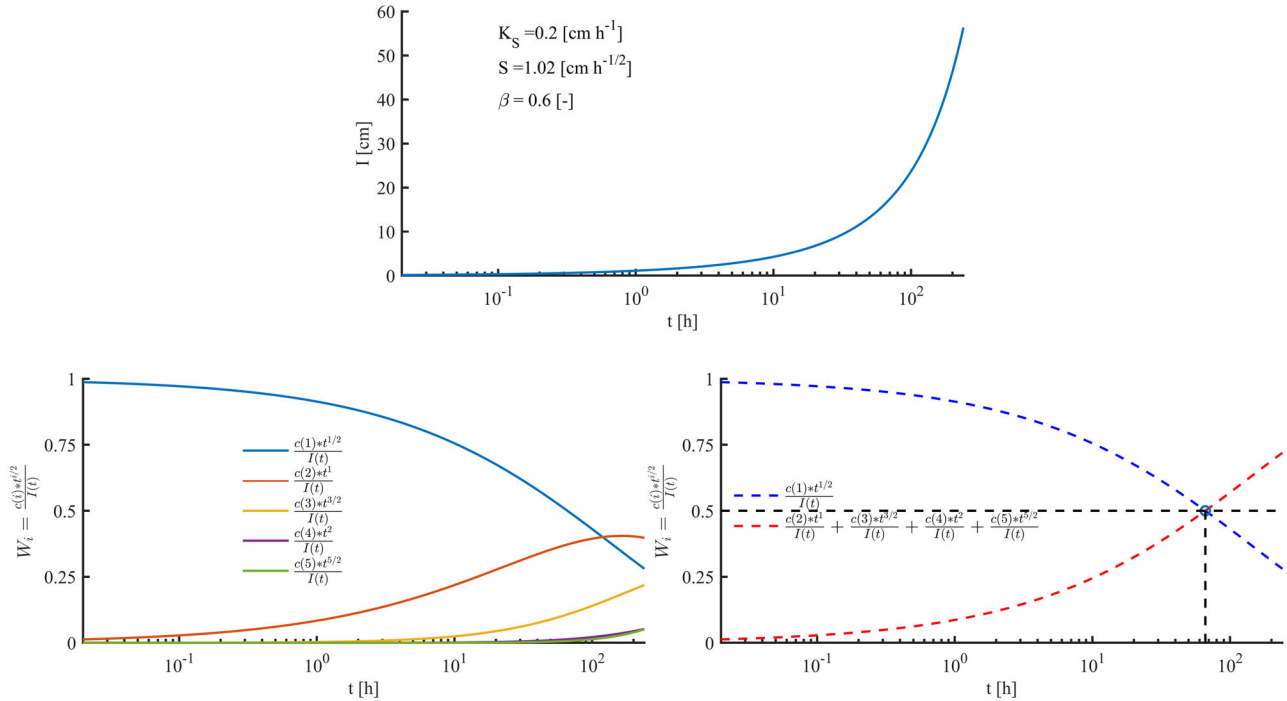
FIGURE 1 The (a) simulated infiltration curve for known values of soil sorptivity (S) and saturated hydraulic conductivity (K_s), (b) temporal variations of the contributions (W) of different terms of the five-term equation to the infiltration process, and (c) temporal variations of the first term contribution vs. the contribution of remaining terms. The β is an integral infiltration constant, t is time, I is cumulative infiltration data, W is the contribution of the sorptivity and gravity components to the infiltration process, and $c(1)$ to $c(5)$ are constants used in approximate expansions of the Haverkamp et al. (1994) formulation

IV. The contribution of the fourth and higher terms is negligible compared with the contribution of the first three components (Figure 1b), and therefore one can exclude the fourth and fifth components from analysis.

V. The variations of the contributions of the sorptivity and gravity components vs. time are symmetric (Figure 1c). This means that by advancing in time, any decrease in the contribution of sorptivity component results in a corresponding increase in the contributions of the gravity components.

VI. When the contribution of the sorptivity (or gravity) component vs. time is plotted, an exponential form of below is obtained (Figures 1b and 1c):

$$W = e^{\alpha t} \qquad (13)$$

where α (h^{-1}) is a soil-dependent shape factor being negative for the sorptivity component and positive for the gravity component.

As a consequence of above facts, once t_{grav} has been identified, the S and K_s can be estimated from the cumulative infiltration data using the iterative procedure below.

2.2 | CTM-I: Iterative procedure to estimate S and K_s

CTM-I is the first part of the CTM method. It considers a given characteristic time (t_{char}) falling between zero and t_{grav} with its related weight, ω:

$$\begin{aligned} \text{at } 0 < t_{char} \leq t_{grav} &\Rightarrow W_1 = 1 - \omega \\ &\Rightarrow \frac{S\sqrt{t_{char}}}{I_{char}} = 1 - \omega \end{aligned} \qquad (14)$$

where $1 - \omega$ is the contribution of the first component to the infiltration process, and I_{char} is the cumulative infiltration at time equal to t_{char}. In the above equation, if t_{char} is equal to t_{grav} ($t_{char} = t_{grav}$), ω will be equal to 0.5. For $t_{char} < t_{grav}$, smaller values of ω will be applied, whereas for $t_{char} \approx 0$, $\omega = 0$ will be applied. The t_{char} can be related to t_{grav} in the following manner:

$$t_{char} = \kappa t_{grav}, \quad \text{where } 0 < \kappa \leq 1 \qquad (15)$$

Rearranging Equation 14 leads to the final solution for S, enabling us to predict S from the knowledge of t_{char}:

$$S = (1 - \omega)\frac{I_{char}}{\sqrt{t_{char}}} \qquad (16)$$

Considering that W_4 and W_5 in Equation 12 are negligible in comparison with $W_2 + W_3$ (Figure 1c), ω corresponds with $W_2 + W_3$, leading to

$$\text{at } 0 < t_{\text{char}} \leq t_{\text{grav}} \Rightarrow W_2 + W_3 = \omega$$
$$\Rightarrow \frac{c(2)t_{\text{char}} + c(3)t_{\text{char}}^{3/2}}{I_{\text{char}}} = \omega \tag{17}$$

where $c(2)$ and $c(3)$ are defined as below:

$$\begin{aligned} c(2) &= \frac{2-\beta}{3}K_s \\ c(3) &= \left(\beta^2 - \beta + 1\right)\frac{K_s^2}{9S} \end{aligned} \tag{18}$$

The rearrangement of Equation 17 based on K_s leads to the following equation:

$$aK_s^2 + bK_s + c = 0 \tag{19}$$

where

$$\begin{aligned} a &= \frac{1}{9(1-\omega)}\left(\beta^2 - \beta + 1\right)\frac{t_{\text{char}}^2}{I_{\text{char}}} \\ b &= \frac{2-\beta}{3}t_{\text{char}} \\ c &= -\omega I_{\text{char}} \end{aligned} \tag{20}$$

where β can be fixed at 0.6 (Haverkamp et al., 1994). Finally, solving for K_s in Equation 19 gives

$$K_s = \frac{-b + \sqrt{b^2 - 4ac}}{2a} \tag{21}$$

where a, b, and c are defined as above.

In order to use Equations 16 and 21, one only needs to estimate from infiltration data the $t_{\text{char}} - I_{\text{char}}$ set as well as ω. The following iterative procedure is applied to determine the $t_{\text{char}} - I_{\text{char}}$ set and ω from field- or laboratory-measured 1D infiltration data in order to compute S and K_s. The procedure is based on the fact that when estimated t_{char} ($t_{\text{char,est}}$) is misestimated, the plot of the first weight W_1 leads to inconsistent values in the vicinity of $t = 0$. In the case of underestimation of t_{char}, W_1 tends towards a value <1, whereas in the case of overestimation of t_{char}, W_1 tends towards a value >1 (see illustrative examples in Figure 2). This implies that a correct estimate of t_{char} can be found by equaling t_{char} to the different values of the observed times (from cumulative infiltration measurements) and selecting $t_{\text{char,est}}$, for which $W_{\text{est}}(t=0)$ converges to 1.

The proposed procedure (Figure 3) aims at determining precisely the right t_{char} with its cumulated infiltration, I_{char}, and weight $1 - \omega$.

Step 1: Set $k = 1$ and ω equal to 0.5, meaning that $t_{\text{char}} = t_{\text{grav}}$ as a first choice.
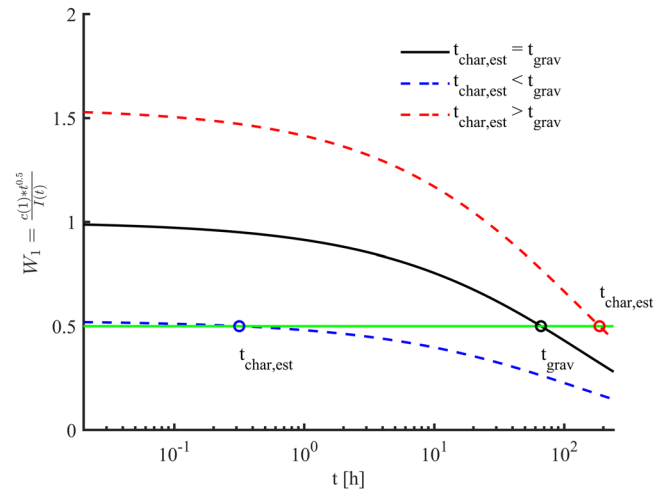
FIGURE 2 The temporal variations of the first component's contribution estimated using different characteristic time (t_{char}) values. This plot is obtained by setting t_{char} to values lower than gravity time (t_{grav}), equal to t_{grav}, and larger than t_{grav} and then by calculating the contribution of the sorptivity component at each data point of time series of analytically generated infiltration data and plotting it vs. time. The t is time, I is cumulative infiltration data, W_1 is the contribution of the sorptivity component to the infiltration process, and $c(1)$ is the constant used in approximate expansions of the Haverkamp et al. (1994) formulation

Step 2: Set $t_{\text{char}}(k)$ and $I_{\text{char}}(k)$ equal to $t(k)$ and $I(k)$ of the infiltration measurement and estimates preliminary value of $S(k)$ using the following equations:

$$S(k) = (1-\omega)\frac{I_{\text{char}}(k)}{\sqrt{t_{\text{char}}(k)}} \tag{22}$$

Step 3: Compute the contribution of the sorptivity (W_1) component for all data points in the time series as follows:

$$W_1(t) = \frac{S(k)\sqrt{t}}{I(t)} \tag{23}$$

Step 4: Determine the maximum value of W_1. Theoretically, if $t_{\text{char}}(k)$ and $I_{\text{char}}(k)$ are set correctly, the maximum W_1 should be equal or very close to 1. Otherwise, maximum W_1 will be lower or higher than 1. To increase the flexibility of the procedure, we define the following criteria as a selection index:

$$1 - d \leq \max(W_1) \leq 1 + d \tag{24}$$

where d is a positive value between 0 and 1. The lower the value of d, the more precise the estimations. In our case, a d value of 0.001 is used to obtain results with the required precision (i.e., 10^{-3}). In the case of noisy experimental infil-
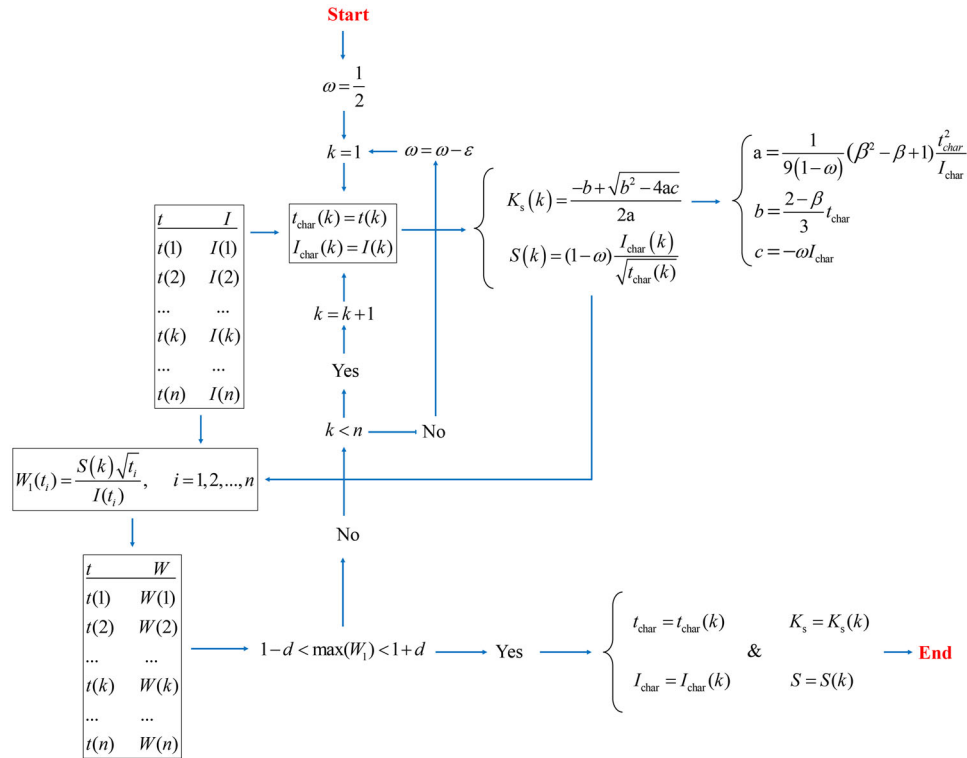
FIGURE 3 A flowchart illustrating the characteristic time method coupled with the iterative procedure (CTM-I) to find the characteristic time (t_{char}) and its corresponding cumulative infiltration value (I_{char}) and to predict soil sorptivity (S) and saturated hydraulic conductivity (K_s). The recommended value for both flexibility constants of ε and d is 0.001. The β is an integral infiltration constant, t is time, I is cumulative infiltration data, and W_1 and ω, respectively, are the contributions of the sorptivity and gravity components to the infiltration process.

tration data, this criterion may be too low, and one may need to widen the range defined in Equation 24 by using higher values of d (e.g., a d value of 0.05 or 0.1 is proposed).

If the criterion of Equation 24 is achieved, end the process by finalizing the $t_{char} - I_{char}$ set and calculate the final solutions for S and K_s using Equations 16 and 21. Otherwise, proceed to Step 5.

Step 5: Set $k = k + 1$ and $t_{char}(k) = t(k)$ and $I_{char}(k) = I(k)$ and estimate updated value of $S(k)$ using Equation 22.

Step 6: Repeat Steps 3–5 until the criterion defined in Equation 24 is achieved, allowing to select the right value of the index $k \leq N$ (N is the number of observed datapoints). If a value of k can be found for $\omega = 0.5$, it means that the observed infiltration data encompasses t_{grav} and describes both the transient and the steady states. Otherwise, if Equation 24 is never fulfilled with W_{est} ($t = 0$) = 1, it means that the t_{grav} value is larger than the maximum time, $t(N)$, and that the observations describe the transient state only. In this case, ω needs to be reduced and Steps 2–6 need to be repeated until t_{char} is found within the measurement time window [$t_{char} \leq t(N)$]. It is recommended to decrease ω by removing small increment (e.g., 0.001) from 0.5 to the appropriate value.

2.3 | CTM-K_s: A procedure for accurate estimation of K_s

It is demonstrated and discussed in Section 4 that CTM-I always provides accurate predictions for S but fails to provide accurate prediction for K_s when the final $\omega < 0.5$. In that case, the following CTM-K_s procedure must be applied for correct predictions of K_s. To this end, the prediction of S from CTM-I (S_{CTM-I}) is used to compute the true contribution of the first component as follows:

$$W_1(t) = \frac{S_{CTM-I}\sqrt{t}}{I(t)} \tag{25}$$

Then, with known time ($\mathbf{t}$) vector from experimental/simulated infiltration data and contribution ($\mathbf{W}_1$) vector from above, one can fit the Equation 13 [which is $W_1 = \exp(\alpha t)$] on $\mathbf{t}$–$\mathbf{W}$ set to predict α (<0). Then, the predicted α value can be used to determine t_{grav} for which $W_1 = 1/2$:

$$t_{grav} = \frac{\ln(0.5)}{\alpha} \tag{26}$$

CTM-I
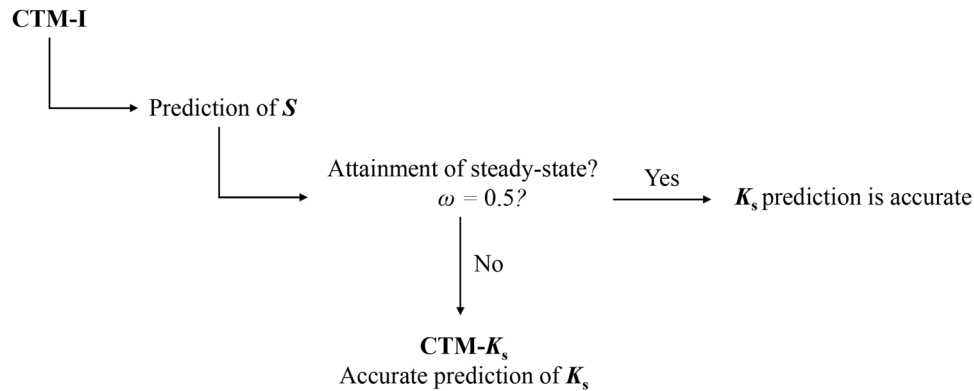
FIGURE 4 A flowchart illustrating the usage of the characteristic time method (CTM) for accurate predictions of both soil sorptivity (S) and saturated hydraulic conductivity (K_s) parameters. ω is the contribution of the gravity component to the infiltration process

Then, one could calculate I_{grav} by rearranging the Equation 13 and putting $W = 0.5$ as below:

$$I_{grav} = \frac{S_{CTM-I}\sqrt{t_{grav}}}{0.5} \tag{27}$$

Finally, when t_{grav} and I_{grav} values were predicted as above, Equation 21 can be used to determine K_s by setting $\omega = 0.5$, $t_{char} = t_{grav}$, and $I_{char} = I_{grav}$.

Figure 4 briefly shows the flowchart of how CTM-I and CTM-K_s should be used to ensure accurate prediction of both S and K_s.

A script written in Python applying the CTM is provided as supplemental material. The Appendix also provides the script in text format. A script written in MATLAB or scilab also could be provided upon to request.

3 | MATERIALS AND METHODS

3.1 | Numerically simulated test data

3.1.1 | Numerical simulations with HYDRUS-1D

To test the proposed procedure, synthetic infiltration curves were simulated by using HYDRUS-1D (Šimůnek, van Genuchten, & Šejna, 2008, 2016) for 12 USDA soil textural classes for a period of 240 h to reach the steady state for most soils. The average soil hydraulic parameters of the van Genuchten–Mualem (VGM) (van Genuchten, 1980) model for each textural class (Table 2) were obtained from the HYDRUS-1D soil catalog (Carsel & Parrish, 1988). A pressure head (equal to zero) boundary condition was imposed at the soil surface, and a free drainage boundary condition was specified at the bottom of the soil profile.

The 200-cm-deep soil profile was assumed homogeneous and was discretized into 401 nodes. Since the profile discretization may affect the numerical results, the accuracy of the time and space discretization was tested against the analytical solution for infiltration without gravity, which is based on the Boltzmann transform. To do this, we simulated water content profiles for 20 different times between 0.01 and 240 h using different spatial resolutions for the profile discretization. Then, water contents were plotted against the Boltzmann variable λ as defined in the following equation (Philip, 1969a):

$$\lambda(\theta) = Z(\theta, t)t^{-1/2} \tag{28}$$

where $Z(\theta,t)$ is a characteristic function, which quantifies the depth at which the volumetric water content equates to θ at time t during an infiltration event under gravity-free conditions (or during horizontal water absorption). In the case of accurate numerical simulations, all θ vs. λ curves at different times should coalesce on one curve. We tested several spatial discretization scenarios and achieved the highest accuracy by applying a spatial resolution of 10^{-6} cm for the first node and gradually increasing the resolution with depth up to a spatial resolution of 1 cm for the last node. We also adjusted the initial time steps in order to achieve the convergence during numerical simulations.

The internal interpolation tables of HYDRUS-1D were disabled to increase the precision of simulated results. A modified VGM model with an air-entry value of -2 cm was used for soils with the n parameter smaller than 1.2. This has been recommended in the literature (Schaap & van Genuchten, 2006; Vogel & Cislerova, 1988; Vogel, van Genuchten, & Cislerova, 2000) in order to avoid an unrealistically sharp decrease of the VGM hydraulic conductivity function close to saturation.

TABLE 2 Average soil hydraulic parameters for the van Genuchten (1980) model for 12 USDA textural classes (Carsel & Parrish, 1988) and the sorptivity (S) value obtained from the horizontal infiltration simulation

Textural class	θ_r	θ_s	θ_i	α	n	m	K_s	S	β
	———cm³ cm⁻³———			cm⁻¹			cm h⁻¹	cm h⁻¹/²	
Clay	0.068	0.380	0.008	1.09	0.083	0.271	0.20	1.02	1.92
Clay loam	0.095	0.410	0.019	1.31	0.237	0.150	0.26	1.46	1.58
Loam	0.078	0.430	0.036	1.56	0.359	0.088	1.04	2.20	1.27
Loamy sand	0.057	0.410	0.124	2.28	0.561	0.057	14.6	6.22	0.80
Sand	0.045	0.430	0.145	2.68	0.627	0.045	29.7	9.23	0.60
Sandy clay	0.100	0.380	0.027	1.23	0.187	0.170	0.12	0.79	1.70
Sandy clay loam	0.100	0.390	0.059	1.48	0.324	0.111	1.31	1.61	1.36
Sandy loam	0.065	0.410	0.075	1.89	0.471	0.066	4.42	3.84	0.99
Silt	0.034	0.460	0.016	1.37	0.270	0.090	0.25	1.35	1.50
Silt loam	0.067	0.450	0.020	1.41	0.291	0.104	0.45	1.66	1.44
Silt clay	0.070	0.360	0.005	1.09	0.083	0.266	0.02	0.35	1.92
Silty clay loam	0.089	0.430	0.010	1.23	0.187	0.197	0.07	0.53	1.70

Note. θ_i, θ_s, and θ_r are initial, saturated, and residual water contents, respectively; α, n, and m are parameters of van Genuchten's (1980) model; K_s is saturated hydraulic conductivity, S is soil sorptivity, and β is an infiltration constant defined by Haverkamp et al. (1994)

3.1.2 | Soil sorptivity inference

In order to test the estimated S values obtained using different methods analyzed in this paper, we needed to know their true values for each examined soil. Rather than using simplified equations to estimate S, we integrated $\lambda(\theta)$ curves numerically simulated by HYDRUS-1D for infiltration without gravity and calculated the S values using the following equation (Philip, 1969a):

$$S = \int_{\theta_i}^{\theta_s} \lambda(\theta) d\theta \qquad (29)$$

where θ_i [L³ L⁻³] and θ_s [L³ L⁻³] are the initial and saturated volumetric water contents, respectively, and $\lambda(\theta)$ [L T⁻¹/²] is the so-called Boltzmann variable defined in Equation 28. The obtained values of S are reported in Table 2.

3.2 | Model comparisons

We compared four different methods, including the characteristic time method (CTM) as proposed above, the Sharma et al. (1980) method (SH), and a nonlinear curve-fitting method (Bonell & Williams, 1986; Bristow & Savage, 1987; Marquardt, 1963; Vandervaere et al., 2000) with two- (CF2, Equation 5) and three-term (CF3, Equation 7) equations, regarding their ability to estimate K_s and S.

In the case of SH method, we used simulated and measured infiltration data lasting for <30 min to estimate S.

The 30 min is selected as a critical time to ensure the linear relationship between I and $\sqrt{t}$ at initial time steps. Therefore, the I was linearly plotted vs. $\sqrt{t}$ for data points obtained between start and 30 min. Then, the slope provides S when intercept is set to zero. For K_s predictions by SH method, we set it to be $K_s = (I_{end} - I_{end-1})/(t_{end} - t_{end-1})$. In the case of CF2 and CF3, the "lsqnonlin" function is used to predict S and K_s.

We truncated simulated infiltration curves to obtain infiltration curves of different durations from 5 min to 10 h, corresponding to a typical infiltration measurement window derived from the Soil Water Infiltration Global (SWIG) database (Rahmati, Weihermüller, Vanderborght, et al., 2018; Rahmati, Weihermüller, & Vereecken, 2018). We used a variable infiltration duration in order to assess the capability of CTM in finding the characteristic time and infiltration independently of the duration of the infiltration experiments.

In addition to the analysis mentioned above, we also used synthetic data with measurement noise as well as experimental data selected from SWIG database (Rahmati, Weihermüller, Vanderborght, et al., 2018; Rahmati, Weihermüller, & Vereecken, 2018) to verify the results obtained from perfect and error-free infiltration data obtained from numerical simulation by HYDRUS-1D.

In the case of data with measurement noise, we first assumed that the water level in the system can be measured with an accuracy of 1 mm, in accordance with most experimental devices and protocols. We account for this by rounding up the simulated cumulative infiltration data expressed in centimeters to one digit after the comma. We

then selected the infiltration times corresponding to each millimeter increment until the whole cumulative infiltration. The cumulative infiltration (I) curve was then differentiated with respect to time to obtain the infiltration rate (**i**). Then we added random noise on the infiltration rates using following equation:

$$\mathbf{i}_{\text{noised}} = \mathbf{i} + r\boldsymbol{\sigma} \tag{30}$$

where $\mathbf{i}_{\text{noised}}$ is the noised infiltration rate vectors, r is a random number between −1 and 1 picked from normal distribution, and $\boldsymbol{\sigma}$ is the vector of standard deviations. We calculated the standard deviation as a function of the nominal values of the infiltration rate **i**, leading to

$$\boldsymbol{\sigma} = e\mathbf{i} \tag{31}$$

where e is the magnitude of error considered in analysis. We used three different values of 0.05, 0.1, and 0.2 indicating an error of 5, 10, and 20%, respectively. Since the range of r in Equation 30 is −1 and 1, a value of $e = 1$ will impose 100% error in each point. Therefore, the parameter e is used to control the maximum allowed error. Finally, after calculating the infiltration rates containing noise ($\mathbf{i}_{\text{noised}}$), we calculated the noised cumulative infiltration (I_{noised}) curve by integration:

$$I_{\text{noised}}(j) = I_{\text{noised}}(j-1) + \mathbf{i}_{\text{noised}}(j)[t(j) - t(j-1)],$$
$$j = 1, \ 2, \ \dots, \ n \tag{32}$$

By applying the above procedure, we are able to propagate the error and generate more "realistic" time series that correspond better with the measurement process. The error was first defined for the infiltration rate and then propagated to the cumulative infiltration. This approach only considers the measurement error and not errors caused by violation of the underlying theoretical assumptions such as the presence of soil layering, nonuniform infiltration, and infiltration in (dead-end) macropores.

In the case of experimental data, we selected 1D infiltration data available in the SWIG database obtained from infiltration experiments using a zero-water potential imposed at surface. In overall, 614 infiltration data were selected for final analysis. As no independent measurements of K_s and S are reported in SWIG for the selected data, we estimated these values using the QEI formulation (Latorre et al., 2015), which we consider as a benchmark for comparison with the estimates from other approaches. It should be noted the QEI is an implicit formulation that slows down the computations and then the predictions of K_s and S.

3.3 | Evaluation of the estimated hydraulic parameters

The accuracy of the CTM and other selected methods was evaluated using the RMSE and Nash and Sutcliffe (1970) efficiency, E, criteria between measured and predicted K_s and S values:

$$\text{RMSE} = \sqrt{\frac{\sum \left(X_{\text{m}} - X_{\text{p}}\right)^2}{n}} \tag{33}$$

$$E = 1 - \frac{\sum \left(X_{\text{m}} - X_{\text{p}}\right)^2}{\sum \left(X_{\text{m}} - \bar{X}_{\text{m}}\right)^2} \tag{34}$$

where X_{m} and X_{p} are the logarithmic values of known and predicted parameters (S and/or K_s), respectively. In the case of the SWIG database, the predictions provided by the QEI model were considered as the known values. The values of RMSE near zero denote a great accuracy, whereas E takes values in the interval $[-\infty, 1]$. A value of E equal to unity shows a perfect match and an E value of zero means that the average of the observed values is as good as predicted values. Negative E values mean that the model is worse for prediction than taking only the mean of the observed values. E values higher than 0.9 show that the slope between observed and predicted values is near unity.

4 | RESULTS AND DISCUSSION

4.1 | CTM for infiltration data in the transient and steady-state infiltration regimes

In order to evaluate the accuracy of the CTM for infiltration data in transient and steady-state infiltration regimes, we applied it on all 12 synthetic soils with infiltration times of 240 h. We evaluated the procedure by comparing the estimated K_s and S values obtained from CTM with their known values and calculated the RMSE and E metrics (Figure 5). The proposed procedure showed very high accuracy in predicting both S and K_s, respectively, with RMSE values of 0.04 cm h$^{-1/2}$ and 0.05 cm h^{-1}, and E values of 0.992 and 0.999 (Figure 5).

As seen from Table 3, all simulated infiltration curves except for silty clay soil predicted t_{char} values with ω value of 0.5. The silty clay soil had ω value of 0.246, indicating that t_{grav} for this soil is higher than the duration of the simulated infiltration curves (532 vs. 240 h, Table 3). Therefore, excluding silty clay soil, the CTM-I is used to predict K_s for
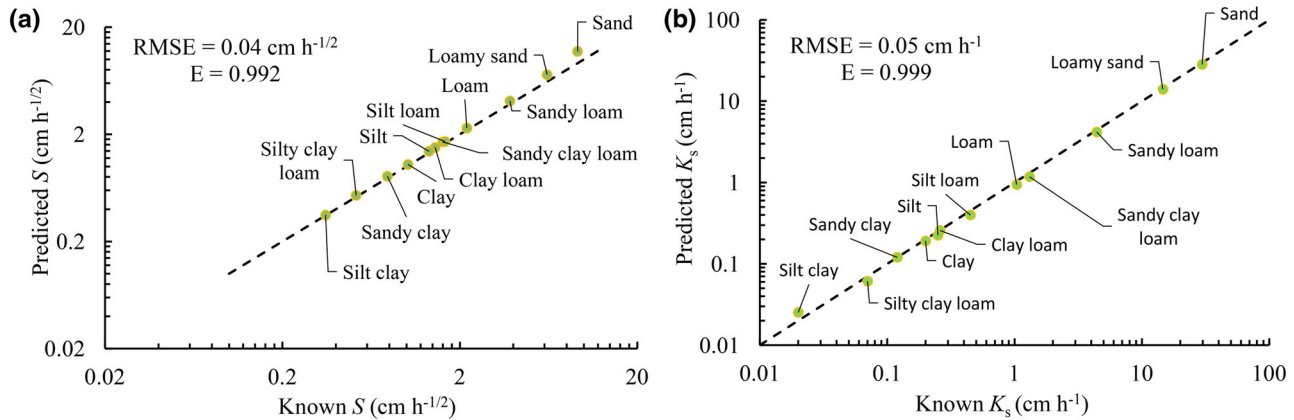
FIGURE 5 Comparison between known and predicted values of soil sorptivity (S) and saturated hydraulic conductivity (K_s) of examined soils using the characteristic time method (CTM) on simulated infiltration curves with 240-h duration. E is the Nash–Sutcliffe efficiency

TABLE 3 Applied values of ω (the contribution of the gravity component to the infiltration process), as well as obtained characteristic (t_{char}) and gravity (t_{grav}) times and the soil-dependent shape factor of α obtained from application of characteristic time method (CTM) over simulated infiltration curves with 240-h duration

Soil	ω	α	t_{char}	t_{grav}
		h^{-1}	——h——	
Clay	0.500	−0.009	81	81
Clay loam	0.500	−0.007	93	93
Loam	0.500	−0.032	16	16
Loamy sand	0.500	−0.600	0.72	0.72
Sand	0.500	−1.032	0.48	0.48
Sandy clay	0.500	−0.006	124	124
Sandy clay loam	0.500	−0.068	5.67	5.67
Sandy loam	0.500	−0.174	2.60	2.60
Silt	0.500	−0.006	104	104
Silt loam	0.500	−0.011	50	50
Silt clay	0.242	−0.001	239	532
Silty clay loam	0.500	−0.003	212	212
Avg.	0.500	−0.162	77	102

The shape factor α values were easily obtained with excellent fits to Equation 13 and considering the full infiltration curves with both the transient and the steady-state infiltration regimes, except for silty clay soil. The corresponding values are reported in Table 3. It is obvious from Table 3 that α values are soil dependent, with smaller values for coarser textured soils. There are very high correlations between α values and known values of S (with Pearson correlation of −.975) and K_s (with Pearson correlation of −.997). Extra research is needed to investigate the nature of the α parameter which is beyond the scope of the current paper.

4.2 | Evaluating the CTM as a function of the expriment duration

In order to evaluate the accuracy of CTM in estimating K_s and S from infiltration measurements that do not necessarily reach the steady-state regime, we applied the method on truncated infiltration curves with different times. We limited the simulated infiltration time to be <24 h because infiltration measurements are usually performed in shorter times, typically up to a few hours. We therefore expect that the steady-state regime is not obtained in most real-world experiments requiring the use of the CTM-K_s procedure.

The outcomes demonstrate very high accuracy of the CTM in the case of S predictions showing an average E value of about unity (0.992 ± 0.0001) and average RMSE value of 0.041 ± 0.0002 cm h$^{-1/2}$, and that the obtained accuracy does not depend on the duration of infiltration, which is already understandable from very small value of standard deviations (with SD values of 0.0001 and 0.0002 for E and RMSE, respectively). The reason why CTM results in very high and time-independent accuracy in the

all soils. In the case of silty clay soil, CTM-K_s is used to provide accurate prediction for K_s. The differences between CTM-I and CTM-K_s is investigated in Section 4.2 applying different infiltration times where the attainment of the steady-state regime in infiltration data is not guaranteed and the use of CTM-K_s is necessary.
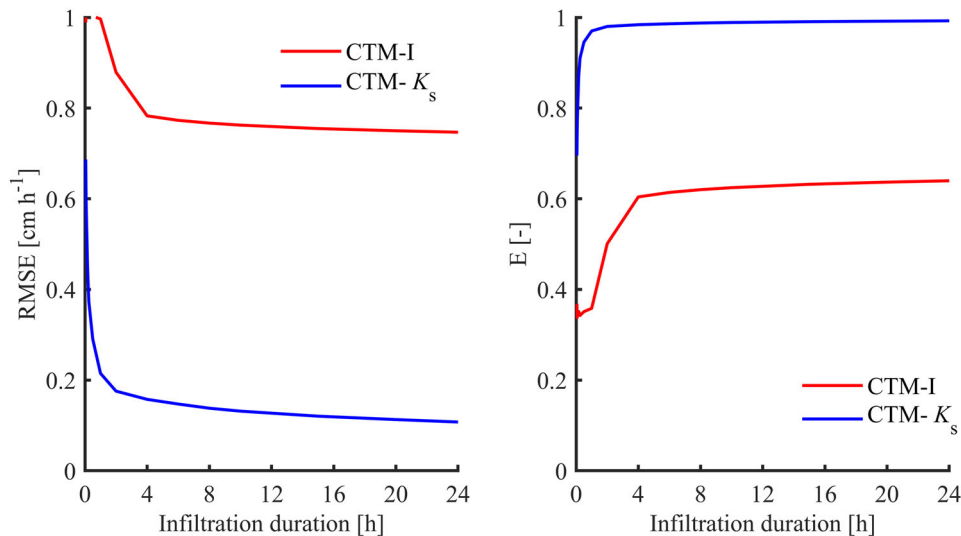
Note that the reported t_{grav} values (Table 3) show that coarse-textured soils have low values of t_{grav}, whereas fine-textured soils have higher values of t_{grav}, which is in line with the physics of water infiltration into soils (with more capillarity-driven flow in fine-textured soils).
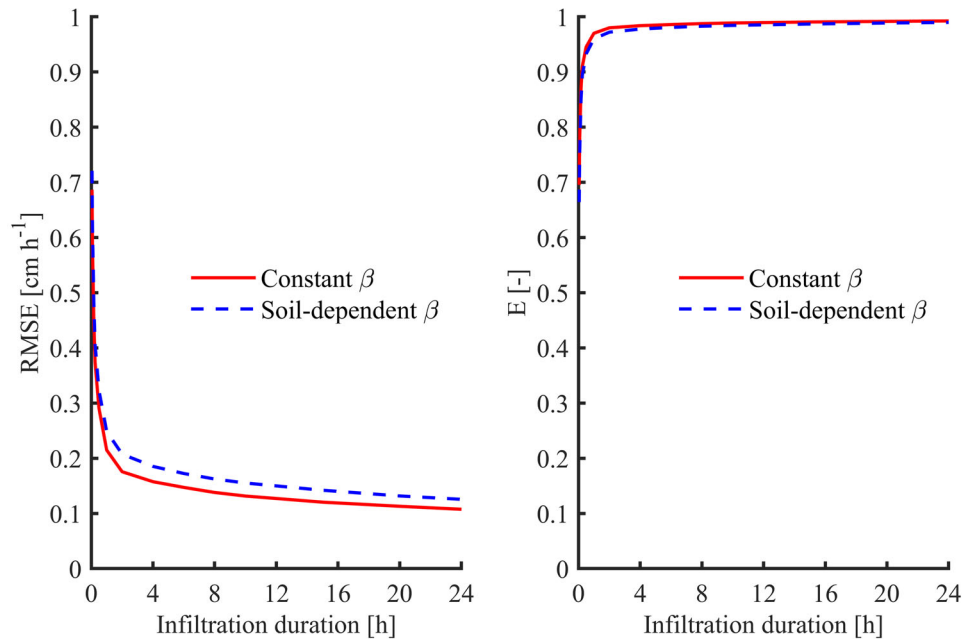
FIGURE 6 Variations of soil-averaged RMSE and Nash–Sutcliffe efficiency (E) criteria of predicted saturated hydraulic conductivity (K_s) over different infiltrations durations using the characteristic time method coupled with the iterative procedure (CTM-I) and the CTM coupled with the K_s procedure (CTM-K_s)

case of S predictions is that CTM relies on the contribution of the first component for S predictions, which is already dominant at initial time steps. Therefore, as soon as enough information to retrieve S from infiltration data is provided at initial time steps, the further times steps will not be necessary for calculation.

Contrary to S, CTM-I fails to predict K_S accurately when using a ω value smaller than 0.5 ($t_{char} < t_{grav}$)(Figure 6). Figure 6 shows that for ω values between 0 and 0.5, K_s prediction was completely dependent on infiltration time, leading to inaccurate estimates for shorter infiltration times and moderately accurate estimates for longer infiltration times. On the other hand, using an iterative procedure (CTM-I), accurate predictions of K_S in fine-textured soils required infiltration times >24 h, which makes the method impractical. This happens because the iterative procedure is developed based on the calculation of the contributions of the sorptivity and gravity terms to the infiltration process and their usage for S and K_S predictions. In fact, the procedure uses the contribution of the sorptivity term to predict S and then the contribution of the gravity terms to predict K_S. Thus, with infiltration data lasting for short times (couple of minutes), the variation of sorptivity contribution occurs around one while at the same time the variation of the contribution of the gravity terms occurs around zero (see Figure 1c). Particularly in the case of fine-textured soils, the contribution of gravity terms stays around zero for a longer period, preventing the procedure from accurate prediction of the K_S. In other words, the iterative procedure requires

obtaining infiltration data for a steady state, which may take a very long to attain (see Lassabatere, Angulo-Jaramillo, Soria-Ugalde, Šimůnek, and Haverkamp (2009) for examples of times required to reach steady state). To overcome this drawback, CTM-K_S was developed to improve K_S predictions for the case of short-time infiltration data. We demonstrate its efficiency for the case of infiltration durations varying between a couple of minutes and 24 h, covering the typical infiltration measurement window (5 min to 10 h for most experiments; Angulo-Jaramillo et al., 2000; Rahmati, Weihermüller, Vanderborght, et al., 2018; Rahmati, Weihermüller, & Vereecken, 2018).

Similar to CTM-I, the CTM-K_S also showed a time-dependent, but high, accuracy for K_S predictions (Figure 6), showing an average E value of 0.921 ± 0.101 and average RMSE value of 0.288 ± 0.205 cm h^{-1}. Exclusion of the infiltration durations shorter than 15 min ($t_{max} < 15$ min) resulted in even higher accuracy and less dependency on infiltration duration in K_S predictions, showing an average E value of 0.975 ± 0.026 and average RMSE value of 0.179 ± 0.084 cm h^{-1}. Thus, we recommend using the CTM-K_S to predict K_S over infiltration data lasting more than 15 min. The recommended duration is within the typical time window of the infiltration measurement (5 min to 10 h). Therefore, when CTM is mentioned hereafter, it refers to use of the CTM-K_S in the case of K_S predictions to ensure accurate prediction. Note that to be applied, CTM-K_S needs a precise estimation of S provided by the previous run of CTM-I, which is always the case.

F I G U R E 7 RMSE and Nash–Sutcliffe efficiency (*E*) criteria obtained between known and predicted saturated hydraulic conductivity (K_s) values using the characteristic time method (CTM) with a constant (β = 0.6) and soil-dependent β parameter over simulated infiltration curves of different durations

## 4.3 | The impact of constant and soil-dependent β on the results of the CTM

Since the CTM is developed based on the approximate expansion of Haverkamp et al. (1994) model involving three input parameters (K_s, *S*, and β), in this section, we aimed to evaluated the remaining β parameter's effects on predictions of *S* and K_s. However, we excluded *S* from this analysis because as seen from Equation 16, β has no effect on *S* predictions. Therefore, we only illustrates the results for K_s predictions in this section. Lassabatere et al. (2009) showed an excellent agreement between the numerically generated infiltration data and the model developed by Haverkamp et al. (1994), provided that the values of β are adapted to the soil type, ranging between values of 0.3 and 1.7 for sand and silt soils, respectively. However, more recent studies (Latorre et al., 2015; Rahmati et al., 2019) proved that the choice of the value of β had only a slight effect on the estimates of *S* and K_s when using Equation 3 and that the default value proposed by Haverkamp et al. (1994) (i.e., 0.6) could be considered as a good option. Therefore, in order to check the effect of a constant or soil-dependent β parameter on the efficiency of CTM in estimating K_s and *S*, we used a constant β value of 0.6 and a soil-dependent β parameter for time-variant infiltration curves (0–24 h). In the case of soil-dependent β, we used Equation 4 to estimate β before deriving K_s and *S* with the CTM method.

In the case of a soil-dependent β parameter, the RMSE and *E* criteria were slightly higher and lower, respectively, compared with the RMSE and *E* values obtained with a constant β (Figure 7), showing average RMSE value of 0.316 vs. 0.288 cm h^{-1} and *E* value of 0.909 vs. 0.921. One might expect better accuracy for a soil-dependent β parameter compared with a constant β. However, this does not happen because, as Lassabatere et al. (2009) has already discussed, Equation 4 does not necessarily provide the best values for soil-dependent β parameter, particularly in the case of fine-textured soils. We conducted the Mann–Whitney–Wilcoxon test to examine whether the use of a constant or soil-dependent β parameter led to differences in K_s estimates. The result (with a *p* value of .75) showed no significant difference between these two approaches, despite significant differences between the computed and default values for β. We therefore recommend the use of CTM with a constant β value of 0.6. Previously Latorre et al. (2018) also showed that the quasi-exact implicit solution of Haverkamp et al. (1994) and its approximate expansions are less sensitive to β.

4.4 | Models comparison using error-free and noised synthetic infiltration curves

To compare CTM with other methods, we examined the gain in accuracy of CTM in estimating *S* and K_s compared
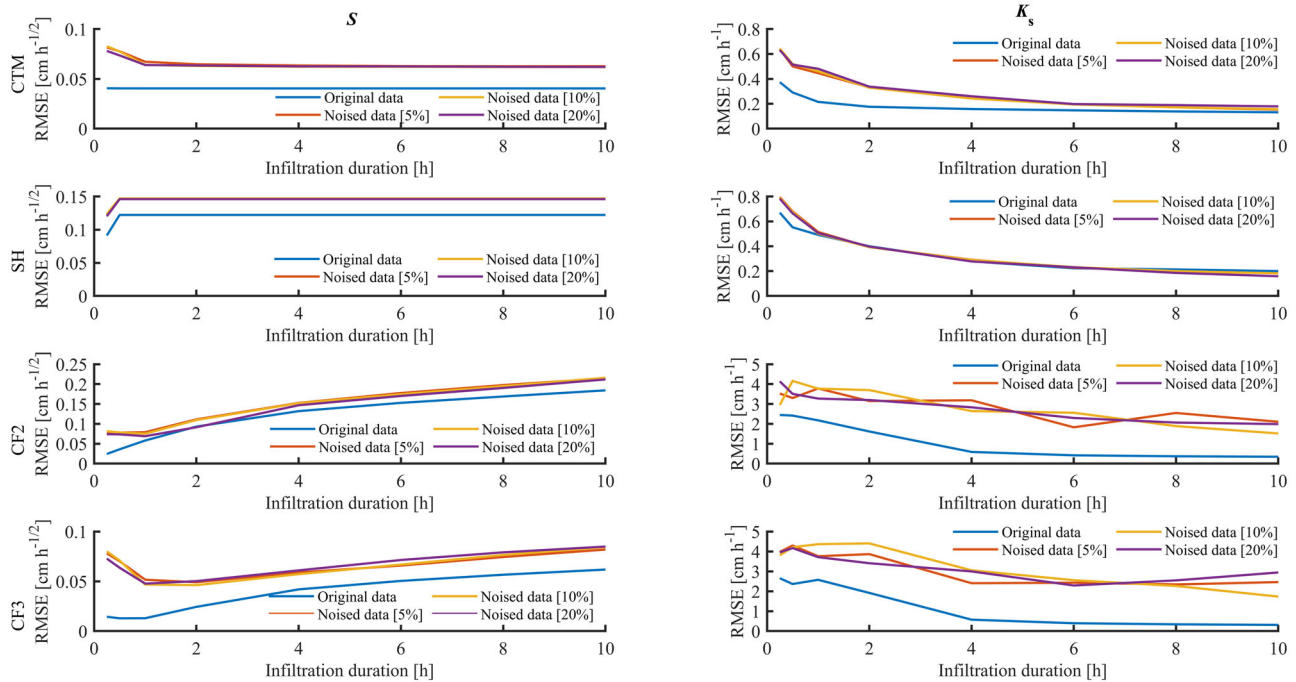
FIGURE 8 Soil-averaged RMSE between logarithms of known and predicted saturated hydraulic conductivity (K_s) (right) and soil sorptivity (S) (left) values using the characteristic time method (CTM), Sharma method (SH), and nonlinear curve fitting methods of two- (CF2) and three-terms (CF3) equations over original and noised synthetic data

with SH, CF2, and CF3. To do this, we used the synthetic infiltration curves with a duration between 15 min and 10 h, corresponding to typical infiltration experiments, as discussed above. In addition to the original error-free data, we also added some random noises over synthetic infiltration data to make them more representative of field conditions and to see the consequences on CTM estimations. Readers are invited to refer Section 3 for the details of noise addition on infiltration data. Figure 8 illustrates the RMSE values obtained between known and predicted values of K_s and S over different times, and Table 4 reports the average values for each method.

Considering the error-free data, the CTM method showed the best performance in estimating both K_s and S showing average RMSE values of 0.204 ± 0.086 cm h^{-1} and 0.040 ± 0.0001 cm h$^{-1/2}$, respectively (Table 4). The SH method showed the lowest performance in estimating the S (with average RMSE values of 0.118 ± 0.011 cm h$^{-1/2}$), whereas it ranked second in estimating the K_s showing an RMSE value of 0.379 ± 0.178 cm h^{-1} (Table 4). The CF2 and CF3 methods showed the lowest performance in the case of K_s estimates, showing RMSE values>1.2 cm h^{-1}. In the case of S estimates, the CF3 was competitive with CTM, showing RMSE values of 0.034 ± 0.020 cm h$^{-1/2}$ vs. 0.040 ± 0.001 cm h$^{-1/2}$ for CTM (Table 4). The CF2 ranked third in the case of S estimations, showing an RMSE value of 0.106 ± 0.062 cm h$^{-1/2}$ (Table 4). Therefore, the results reveal that although SH and CF3 methods show good accuracy

in estimation of K_s and S, respectively, they fail in accurate prediction of the other parameter. This happens while the CTM shows very high accuracy in simultaneous estimation of both S and K_s parameters. The accuracy of both predicted parameters using CTM is nearly time independent, which makes the CTM more practical to apply over infiltration data lasting for a couple of minutes to dozens of hours.

In addition to error-free data, overall, 5, 10, and 20% maximum errors were added on infiltration data, and the noise impact on S and K_s predictions was analyzed. The results (Figure 8, Table 4) revealed that in the case of K_s predictions, the accuracy of the CTM even with noisy data was considerably higher than that of CF2 and CF3, as well as SH, showing average RMSE values of 0.341 cm h^{-1} vs. 0.407 cm h^{-1} in the case of SH and >2.9 cm h^{-1} in the case of CF2 and CF3 methods (Table 4). For S predictions, CTM and CF3 showed similar accuracies, with average RMSE values of 0.07 cm h$^{-1/2}$ (Table 4). The average RMSE values of CF2 and SH are nearly double those of CTM and CF3 (Table 4).

A simple comparison between the error-free and noised data also revealed that CTM works nicely, even with 20% noise on data, showing a slight increase in RMSE values due to noise addition. In contrast with CTM, the accuracy of CF2 and CF3 considerably degrades with increase in noise magnitude (particularly in the case of K_s predictions), whereas the average RMSE value increases from

TABLE 4 Average RMSE between logarithms of known and predicted saturated hydraulic conductivity (K_s) and soil sorptivity (S) values using the characteristic time method (CTM), Sharma method (SH), and nonlinear curve fitting method of two- (CF2) and three-term (CF3) equations over original and noised synthetic data for all soils

Data	Method	K_s	S
		cm h^{-1}	cm h$^{-1/2}$
Error-free data	CTM	0.204 ± 0.086	0.040 ± 0.001
	SH	0.379 ± 0.178	0.118 ± 0.011
	CF2	1.296 ± 0.962	0.106 ± 0.062
	CF3	1.391 ± 1.079	0.034 ± 0.020
Noised data (5%)	CTM	0.335 ± 0.177	0.068 ± 0.007
	SH	0.411 ± 0.232	0.144 ± 0.009
	CF2	2.925 ± 0.694	0.136 ± 0.057
	CF3	3.191 ± 0.851	0.067 ± 0.012
Noised data (10%)	CTM	0.340 ± 0.182	0.067 ± 0.008
	SH	0.408 ± 0.229	0.144 ± 0.008
	CF2	2.897 ± 0.933	0.135 ± 0.056
	CF3	3.299 ± 1.041	0.066 ± 0.015
Noised data (20%)	CTM	0.349 ± 0.173	0.066 ± 0.006
	SH	0.401 ± 0.232	0.143 ± 0.009
	CF2	2.910 ± 0.758	0.128 ± 0.058
	CF3	3.252 ± 0.671	0.066 ± 0.013

TABLE 5 Average RMSE and Nash and Sutcliffe (1970) efficiency (E) criteria between logarithms of known and predicted saturated hydraulic conductivity (K_s) and soil sorptivity (S) values using the characteristic time method (CTM), Sharma method (SH), and nonlinear curve fitting method of two- (CF2) and three-term (CF3) equations over experimental data of the Soil Water Infiltration Global (SWIG) database

Criterion	Method	K_s	S
		cm h^{-1}	cm h$^{-1/2}$
RMSE	CTM	0.298	0.307
	SH	0.202	0.184
	CF2	1.685	1.354
	CF3	1.769	0.279
E	CTM	0.891	0.736
	SH	0.938	0.885
	CF2	−2.490	−4.139
	CF3	−2.844	0.782

around 1.3 cm h^{-1} up to 3.2 cm h^{-1}. Although SH is less accurate than CTM, the results were shown to be stable by increase in magnitude of the noise. In the case of S prediction, the RMSE value over noised data is nearly doubled compared with that of error-free data in both CTM and CF3, regardless of the magnitude of the noise.

4.5 | Evaluating the CTM over experimental data

Up to this point in the study, the CTM method was tested and verified over synthetic data obtained from HYDRUS-1D. Experimental data obtained in field campaigns are usually noisy and not perfect. Although we added some random noises over those synthetic data to evaluate the method performance over the noisy data as well, such a noise addition will not represent other important error sources such as soil layering, nonuniform infiltration, and infiltration in (dead-end) macropores. Therefore, a performance evaluation over experimental data is yet required. However, experimental data usually lack the true values of

S and K_s, making it difficult to evaluate the accuracy of the methods (i.e., the comparison of estimated values against targeted real values). On the other hand, the measured values of K_s mostly occur in disturbed or undisturbed soil samples, which are mostly not representative of field conditions under infiltration measurements. Therefore, the K_s values predicted from infiltration data rarely ever correspond to those values obtained from small soil samples.

As a conclusion of the above, we used field experimental data taken from the SWIG database (Rahmati, Weihermüller, Vanderborght, et al., 2018; Rahmati, Weihermüller, & Vereecken, 2018) to verify the feasibility of the application of the proposed method to real data and the potential impact of experimental noise. In order to cover the lack of the true and benchmark values of the S and K_s, we used QEI formulation of the Haverkamp et al. (1994), which is valid for entire time to be solved numerically to retrieve the benchmark values of S and K_s. Then, we compared the CTM predicted values of S and K_s, as well as those predicted by SH, CF2, and CF3, with the benchmark values. Although the QEI-retrieved values of S and K_s are considered as the most accurate predictions of parameters, it is impractical for routine use because the numerical calculations of the parameters last for couple of hours in most cases.

As shown in Figure 9 and summarized in Table 5, both S and K_s values predicted by CTM are considerably comparable with benchmark values. The CTM showed a RMSE value of 0.202 cm h^{-1} in the case of K_s predictions and 0.307 cm h$^{-1/2}$ in the case of S prediction. The SH method was even more robust compared with CTM, showing RMSE values of 0.202 cm h^{-1} and 0.184 cm h$^{-1/2}$ in the case of K_s and S predictions, respectively. Although, the SH method shows slightly better robustness than CTM,
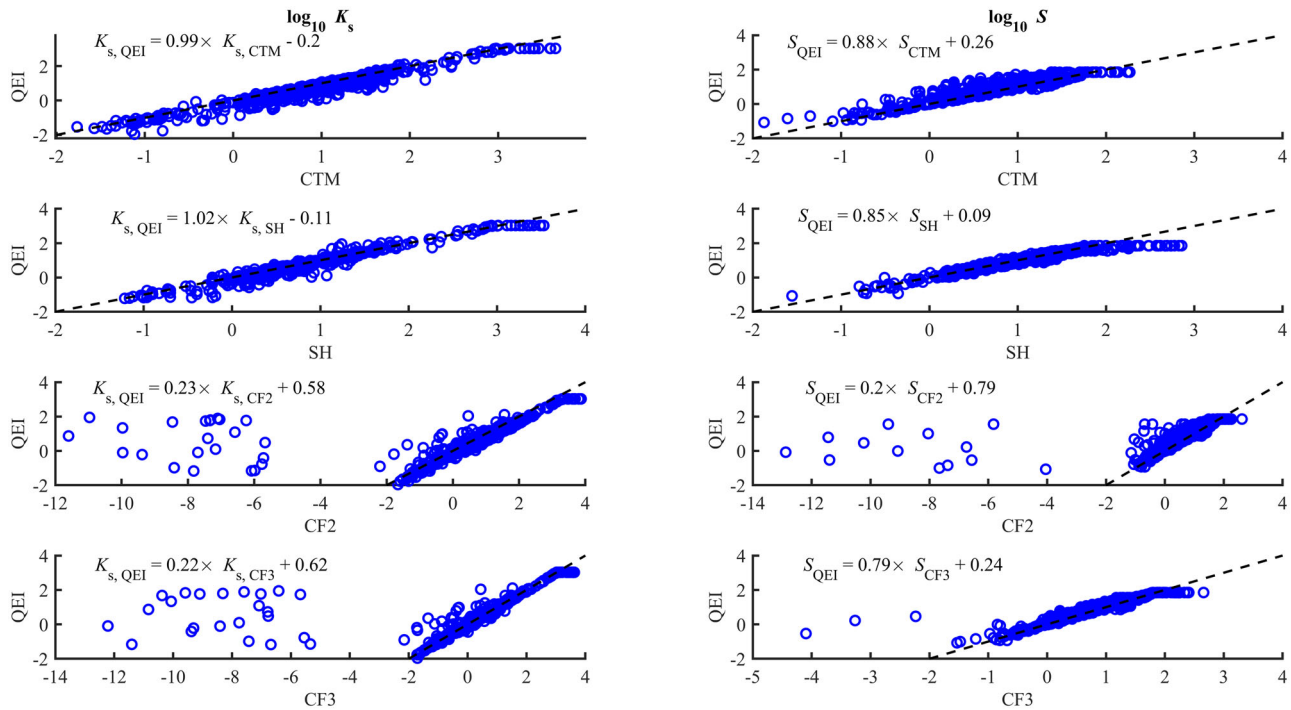
FIGURE 9 Logarithms of predicted saturated hydraulic conductivity (K_s) and sorptivity (S) values using the characteristic time method (CTM) and Sharma et al. (1980) (SH) method, as well as curve fitting methods of two- (CF2) and three-term (CF3) equations vs. logarithms of their most accurate estimates using quasi-exact implicit (QEI) solution of Haverkamp et al. (1994)

it still requires arbitrary selection of the data for accurate prediction of S. When using the SH method, one first needs to decide up to which point of measured data the relationship between I and $t^{1/2}$ is linear, and then the selected part should be used for S predictions. This adds some arbitrariness to S predictions, leading to uncertainty in estimated values depending on the choice made. In our calculations, after several examinations, we finally decided that when a critical time of 30 min is used to separate the first part of data for S predictions, it results in the highest accuracy of the S predictions overall. However, the use of CTM omits the necessity of such arbitrariness in selection, showing very high robustness compared with QEI formulation. Contrary to CTM, SH, CF2, and CF3 show unacceptable accuracy for K_s predictions. Although CF3 shows an accuracy comparable with CTM and SH in the case of S predictions, CF2 fails in this case too. It must be noted that if one excludes the outliers from CF2 and CF3 predictions, the accuracy might be close to that obtained from CTM and SH (Figure 9). However, the outliers reveal that CF2 and CF3 might have physically unconstrained fitting over infiltration data in several cases, which challenges the reliable use of them for S and K_s predictions. This happens while CTM provides physically constrained fitting of data. This could be the case for SH method as well, only in a condition that the separation of the linear part of the infiltration data for S predictions is done correctly.

4.6 | Practical interest of the CTM

The CTM method has several practical advantages since it overcomes several shortcomings encountered when S and K_s are estimated using non-linear curve-fitting methods. It is built on the framework of the approximate expansions of the quasi-exact implicit model developed by Haverkamp et al. (1994), providing the most general and accurate description of 1D water infiltration compared with classical choices based on, for example, Philip (1957) or empirical equations (Holtan, 1961; Horton, 1941; Kostiakov, 1932). In addition, CTM addresses the right physics (i.e., the physics of water infiltration under the fixed water pressure head at the surface, as is the case for regular devices and protocols).

Nonlinear curve fitting methods require an appropriate selection of data, which is complicated since the characteristic time that divides the transient and steady states is unknown and depends on unknown values of S and K_s. To alleviate this problem, iterative procedures were used to select a priori data, estimate values of S and K_s, and then compute the characteristic time to validate the selection posteriori, as done in the Beerkan estimation of soil transfer (BEST) methods (Angulo-Jaramillo et al., 2019). Haverkamp et al. (1994) developed an implicit formulation, which is valid for all times and can be used to invert experimental data (Fernández-Gálvez, Pollacco, Lassabatere, Angulo-Jaramillo, & Carrick, 2019; Latorre

et al., 2015). However, its use is quite complicated due to its implicit feature, and thus direct models (dedicated to either transient or steady-state regimes) are still preferred.

The fit itself requires paying attention to several additional crucial points. The fit involves the choice of an objective function that is barely developed. The objective functions can be of two main types: distance-based or weak form-based functions, with the distance-based functions being the most popular in soil science and hydrology (Guinot, Cappelaere, Delenne, & Ruelland, 2011). Several choices are available among the distance-based objective functions, such as the Nash–Sutcliffe efficiency, the sum of squared errors (SSE), the RMSE, the mean absolute error (MAE), the volumetric efficiency (VE), or the generalized Nash–Sutcliffe efficiency (GNSE) (Guinot et al., 2011). However, little attention is paid to the choice of the right objective function among these options. In addition, these types of functions are known to introduce local minima in the model response, resulting in a strong dependence on the choice of the initial values. The model response and objective functions should be tested to avoid equifinality and nonuniqueness (Pollacco et al., 2013).

The CTM method avoids all these shortcomings outlined above. Its sole complexity involves the use of an iterative process that is necessary since the knowledge of the transition time between transient and steady regime depends on unknown values of S and K_S. Despite this difficulty, no fits are required, and the computation involves only simple algebraic operations. Its adaptation to all types of datasets (encompassing a part of the transient state or including both transient and steady states) makes it a useful tool. In addition to its advantages, our study demonstrates its efficiency in reaching its goal. All these aspects make the CTM method a promising method for the estimation of S and K_S.

5 | CONCLUSIONS

In this paper, we proposed a new method, the characteristic time method (CTM), based on the concept of characteristic time (t_{char}) to estimate the soil sorptivity S and the saturated hydraulic conductivity K_s in a physically constrained manner using the two- and three-term approximate expansion developed by Haverkamp et al. (1994) from cumulative infiltration measurements. The CTM method requires no knowledge of the infiltration duration, for which Philip's (1957) infiltration equation and the two- or three-term equations of Haverkamp et al. (1994) are valid. We analyzed the accuracy of CTM using simulated and experimental infiltration curves and by comparing CTM with methods typically used in the literature, including nonlinear curve fitting of two- (CF2) and three-term (CF3) equations, and the methods proposed by Sharma et al.

(1980) (SH). We used HYDRUS-1D to simulate the synthetic infiltration curves for soils with different textures ranging from sandy to clayey soils. We found that CTM provided accurate predictions of K_S and S compared with the other methods when tested against numerically generated infiltration curves with a duration of couple of minutes to dozens of hours. The accuracy of the CTM was better than other examined methods. The most important advantage of CTM is that it needs no prior knowledge about the time domain validity of the applied equation(s). In contrast, the other methods failed when applied to time-variant infiltration curves. The CTM was found to be applicable to any infiltration duration within a typical time window used for infiltration experiments (5 min to 10 h), and even up to 240 h. The accuracy of K_S and S predictions using CTM showed no dependency on the duration of infiltration. We also evaluated the performance of the CTM in a comparison with other methods over noised synthetic data, as well as experimental data selected from the SWIG database (Rahmati, Weihermüller, Vanderborght, et al., 2018; Rahmati, Weihermüller, & Vereecken, 2018), to verify the usage of the CTM with real noised data. The results showed that even with noised and experimental data, the CTM still was better than CF2 and CF3, showing considerably higher accuracy, particularly in the case of K_S predictions. The CTM method was also comparable with the classical method of SH owing to the advantage of no arbitrariness in selection of data for accurate predictions of S and K_S. Further research is needed to corroborate the estimated values of S and K_S using CTM with independently determined values of S and K_S. Also, improved estimates of S and K_S may prove to be valuable in constraining estimates of the van Genuchten (1980) model's parameters, such as α and n.

CONFLICT OF INTEREST
The authors declare no conflict of interest.

ORCID
Mehdi Rahmati https://orcid.org/0000-0001-5547-6442
Laurent Lassabatere https://orcid.org/0000-0002-8625-5455
Harry Vereecken https://orcid.org/0000-0002-8051-8517

REFERENCES
Angulo-Jaramillo, R., Bagarello, V., Di Prima, S., Gosset, A., Iovino, M., & Lassabatere, L. (2019). Beerkan estimation of soil transfer parameters (BEST) across soils and scales. *Journal of Hydrology*, *576*, 239–261. https://doi.org/10.1016/j.jhydrol.2019.06.007

Angulo-Jaramillo, R., Vandervaere, J. P., Roulier, S., Thony, J. L., Gaudet, J. P., & Vauclin, M. (2000). Field measurement of soil surface hydraulic properties by disc and ring infiltrometers: A review and recent developments. *Soil and Tillage Research*, *55*, 1–29. https://doi.org/10.1016/S0167-1987(00)00098-2

Beven, K., & Freer, J. (2001). Equifinality, data assimilation, and uncertainty estimation in mechanistic modelling of complex environmental systems using the GLUE methodology. *Journal of Hydrology*, *249*, 11–29. https://doi.org/10.1016/S0022-1694(01)00421-8

Bonell, M., & Williams, J. (1986). The two parameters of the Philip infiltration equation: Their properties and spatial and temporal heterogeneity in a red earth of tropical semi-arid Queensland. *Journal of Hydrology*, *87*, 9–31. https://doi.org/10.1016/0022-1694(86)90112-5

Bristow, K. L., & Savage, M. J. (1987). Estimation of parameters for the Philip two-term infiltration equation applied to field soil experiments. *Soil Research*, *25*, 369–375. https://doi.org/10.1071/SR9870369

Carsel, R. F., & Parrish, R. S. (1988). Developing joint probability distributions of soil water retention characteristics. *Water Resources Research*, *24*, 755–769. https://doi.org/10.1029/WR024i005p00755

Fernández-Gálvez, J., Pollacco, J., Lassabatere, L., Angulo-Jaramillo, R., & Carrick, S. (2019). A general Beerkan estimation of soil transfer parameters method predicting hydraulic parameters of any unimodal water retention and hydraulic conductivity curves: Application to the Kosugi soil hydraulic model without using particle size distribution data. *Advances in Water Resources*, *129*, 118–130. https://doi.org/10.1016/j.advwatres.2019.05.005

Green, W. H., & Ampt, G. A. (1911). Studies on soil physics. *Journal of Agricultural Science*, *4*, 1–24. https://doi.org/10.1017/S0021859600001441

Guinot, V., Cappelaere, B., Delenne, C., & Ruelland, D. (2011). Towards improved criteria for hydrological model calibration: Theoretical analysis of distance- and weak form-based functions. *Journal of Hydrology*, *401*, 1–13. https://doi.org/10.1016/j.jhydrol.2011.02.004

Haverkamp, R., Parlange, J. Y., Starr, J. L., Schmitz, G., & Fuentes, C. (1990). Infiltration under ponded conditions: 3. A predictive equation based on physical parameters. *Soil Science*, *149*, 292–300.

Haverkamp, R., Ross, P. J., Smettem, K. R. J., & Parlange, J. Y. (1994). Three-dimensional analysis of infiltration from the disc infiltrometer: 2. Physically based infiltration equation. *Water Resources Research*, *30*, 2931–2935. https://doi.org/10.1029/94WR01788

Holtan, H. N. (1961). *Concept for infiltration estimates in watershed engineering*. Washington, DC: USDA-ARS.

Horton, R. E. (1941). An approach toward a physical interpretation of infiltration-capacity. *Soil Science Society of America Journal*, *5*, 399–417. https://doi.org/10.2136/sssaj1941.036159950005000C0075x

Kostiakov, A. N. (1932). On the dynamics of the coefficient of water percolation in soils and the necessity of studying it from the dynamic point of view for the purposes of amelioration. In *Transactions of 6th Committee International Society of Soil Science* (pp. 7–21). International Society of Soil Science.

Lassabatere, L., Angulo-Jaramillo, R., Soria Ugalde, J., Cuenca, R., Braud, I., & Haverkamp, R. (2006). Beerkan estimation of soil transfer parameters through infiltration experiments: BEST. *Soil Science Society of America Journal*, *70*, 521–532. https://doi.org/10.2136/sssaj2005.0026

Lassabatere, L., Angulo-Jaramillo, R., Soria-Ugalde, J., Šimůnek, J., & Haverkamp, R. (2009). Numerical evaluation of a set of analytical infiltration equations. *Water Resources Research*, *45*(12). https://doi.org/10.1029/2009WR007941

Latorre, B., Moret-Fernández, D., Lassabatere, L., Rahmati, M., López, M. V., Angulo-Jaramillo, R., … Jiménez, J. J. (2018). Influence of the β parameter of the Haverkamp model on the transient soil water infiltration curve. *Journal of Hydrology*, *564*, 222–229. https://doi.org/10.1016/j.jhydrol.2018.07.006

Latorre, B., Peña, C., Lassabatere, L., Angulo-Jaramillo, R., & Moret-Fernández, D. (2015). Estimate of soil hydraulic properties from disc infiltrometer three-dimensional infiltration curve. Numerical analysis and field application. *Journal of Hydrology*, *527*, 1–12. https://doi.org/10.1016/j.jhydrol.2015.04.015

Marquardt, D. W. (1963). An algorithm for least-squares estimation of nonlinear parameters. *Journal of the society for Industrial and Applied Mathematics*, *11*, 431–441. https://doi.org/10.1137/0111030

Moret-Fernández, D., Blanco, N., Martínez-Chueca, V., & Bielsa, A. (2013). Malleable disc base for direct infiltration measurements using the tension infiltrometry technique. *Hydrological Processes*, *27*, 275–283. https://doi.org/10.1002/hyp.9206

Moret-Fernández, D., Latorre, B., & Angulo-Martínez, M. (2017). Comparison of different methods to estimate the soil sorptivity from an upward infiltration curve. *Catena*, *155*, 86–92. https://doi.org/10.1016/j.catena.2017.03.009

Nash, J. E., & Sutcliffe, J. V. (1970). River flow forecasting through conceptual models part I: A discussion of principles. *Journal of Hydrology*, *10*, 282–290. https://doi.org/10.1016/0022-1694(70)90255-6

Parlange, J. Y., Lisle, I., Braddock, R. D., & Smith, R. E. (1982). The three-parameter infiltration equation. *Soil Science*, *133*, 337–341. https://doi.org/10.1097/00010694-198206000-00001

Philip, J. R. (1957). The theory of infiltration: 1. The infiltration equation and its solution. *Soil Science*, *83*, 345–358.

Philip, J. R. (1969a). Moisture equilibrium in the vertical in swelling soils. I. Basic theory. *Soil Research*, *7*, 99–120. https://doi.org/10.1071/SR9690099

Philip, J. R. (1969b). *Theory of infiltration.* Advances in Hydroscience, *5*, 215–296. https://doi.org/10.1016/B978-1-4831-9936-8.50010-6

Pollacco, J. A. P., Nasta, P., Soria-Ugalde, J. M., Angulo-Jaramillo, R., Lassabatere, L., Mohanty, B. P., & Romano, N. (2013). Reduction of feasible parameter space of the inverted soil hydraulic parameter sets for Kosugi model. *Soil Science*, *178*, 267–280.

Rahmati, M., Latorre, B., Lassabatere, L., Angulo-Jaramillo, R., & Moret-Fernández, D. (2019). The relevance of Philip theory to Haverkamp quasi-exact implicit analytical formulation and its uses to predict soil hydraulic properties. *Journal of Hydrology*, *570*, 816–826. https://doi.org/10.1016/j.jhydrol.2019.01.038

Rahmati, M., Weihermüller, L., Vanderborght, J., Pachepsky, Y. A., Mao, L., Sadeghi, S. H., … Vereecken, H. (2018). Development and analysis of the Soil Water Infiltration Global database. *Earth System Science Data*, *10*, 1237–1263. https://doi.org/10.5194/essd-10-1237-2018

Rahmati, M., Weihermüller, L., & Vereecken, H. (2018) Soil Water Infiltration Global (SWIG) database. *PANGAEA*. https://doi.org/10.1594/PANGAEA.885492

Richards, L. A. (1931). Capillary conduction of liquids through porous mediums. *Physics*, *1*, 318–333. https://doi.org/10.1063/1.1745010

Schaap, M. G., & van Genuchten, M. Th. (2006). A modified Mualem–van Genuchten formulation for improved description of the hydraulic conductivity near saturation. *Vadose Zone Journal*, *5*, 27–34. https://doi.org/10.2136/vzj2005.0005

Sharma, M. L., Gander, G. A., & Hunt, C. G. (1980). Spatial variability of infiltration in a watershed. *Journal of Hydrology*, *45*, 101–122. https://doi.org/10.1016/0022-1694(80)90008-6

Šimůnek, J., van Genuchten, M. Th., & Šejna, M. (2008). Development and applications of the HYDRUS and STANMOD software packages and related codes. *Vadose Zone Journal*, *7*, 587–600. https://doi.org/10.2136/vzj2007.0077

Šimůnek, J., van Genuchten, M. Th., & Šejna, M. (2016). Recent developments and applications of the HYDRUS computer software packages. *Vadose Zone Journal*, *15*(7). https://doi.org/10.2136/vzj2016.04.0033

Smiles, D. E., & Knight, J. H. (1976). A note on the use of the Philip infiltration equation. *Soil Research*, *14*, 103–108. https://doi.org/10.1071/SR9760103

Swartzendruber, D. (1987). A quasi-solution of Richards' equation for the downward infiltration of water into soil. *Water Resources Research*, *23*, 809–817. https://doi.org/10.1029/WR023i005p00809

Valiantzas, J. D. (2010). New linearized two-parameter infiltration equation for direct determination of conductivity and sorptivity. *Journal of Hydrology*, *384*, 1–13. https://doi.org/10.1016/j.jhydrol.2009.12.049

van Genuchten, M. Th. (1980). A closed-form equation for predicting the hydraulic conductivity of unsaturated soils. *Soil Science Society of America Journal*, *44*, 892–898. https://doi.org/10.2136/sssaj1980.03615995004400050002x

Vandervaere, J. P., Vauclin, M., & Elrick, D. E. (2000). Transient flow from tension infiltrometers I. The two-parameter equation. *Soil Science Society of America Journal*, *64*, 1263–1272. https://doi.org/10.2136/sssaj2000.6441263x

Vogel, T., & Cislerova, M. (1988). On the reliability of unsaturated hydraulic conductivity calculated from the moisture retention curve. *Transport in Porous Media*, *3*, 1–15. https://doi.org/10.1007/BF00222683

Vogel, T., van Genuchten, M. Th., & Cislerova, M. (2000). Effect of the shape of the soil hydraulic functions near saturation on variably-saturated flow predictions. *Advances in Water Resources*, *24*, 133–144. https://doi.org/10.1016/S0309-1708(00)00037-3

SUPPORTING INFORMATION

Additional supporting information may be found online in the Supporting Information section at the end of the article.

Appendix
The Python code applying the CTM method on infiltration data

```
# Description

# The function finds the S and Ks from infiltration curve supplied in data using CTM procedure

# The DATA is a matrix with two column and n rows providing [t, I]

# Classes

import pandas as pandas # Check if pandas is installed on your system. If not, install it by: pip install pandas –user

import numpy as numpy # Check if numpy is installed on your system. If not, install it by: pip install numpy –user

from scipy.stats import linregress # Check if scipy is installed on your system. If not, install it by: pip install scipy –user

import scipy as scipy # Check if scipy is installed on your system. If not, install it by: pip install scipy –user

# Reading data from EXCEL

File_Location = 'SimulatedData.xlsx' # Change the direction based on your file location

Sheet_Name = 'Clay' # Does the calculation for Clay soil. Change it accordingly

DataLabels = ['T', 'I'] # Change the labels based on your input file.

DATA = pandas.read_excel(File_Location, Sheet_Name)

HEADERs = DATA.columns

NumberOFHeaders = len(HEADERs)

for i in range(NumberOFHeaders):
    DataLabels[i] = DATA[HEADERs[i]]

T = DataLabels[0]

I = DataLabels[1]

T = T[T<=240]
```

```
I = I[0:len(T)]
# Setting initial values
beta  = 0.6 # beta value of Haverkamp model. Change this if you want to use soil-specific value
epsilon = 0.001 # The arbitrary value between zero and 0.5 used to adjust omega. Change it to speed up the procedure
d = 0.001 # An arbitrary value between 0 & 1. Change it to increase the flexibility of the procedure
 # CTM Code
def CTM(T, I, beta):
    t_char, I_char, Sp, Kp1, omega = CTM_I(T, I, beta)
    Kp2, t_grav, I_grav, alpha = CTM_Ks(Sp, t_char, I_char, omega, beta, T, I)
    return Sp, Kp1, Kp2, t_char, I_char, t_grav, I_grav, omega, alpha
# CTM Core Code
def CTM_I(T, I, beta):
    # Default values
    t_char = numpy.nan
    I_char = numpy.nan
    Sp = numpy.nan
    Kp = numpy.nan
    omega = 0.5 + epsilon
    t_char = numpy.nan
    # Calculation
    while numpy.isnan(t_char):
        omega = omega - epsilon
        t_char, I_char, Sp, Kp = Iterative_procedure(T, I, beta, omega)
        if omega <= 0.001:
            break
    return t_char, I_char, Sp, Kp, omega
def Iterative_procedure(T, I, beta, omega):
    # Default values
    t_char = numpy.nan
    I_char = numpy.nan
    Sp = numpy.nan
    Kp = numpy.nan
    # Calculation
    data_lenght = len(T)
    for k in range(1, data_lenght):
        tc = T[k]
        Ic = I[k]
        SS = (1-omega)*(Ic/numpy.sqrt(tc)) # Computes a preliminary stimate for S
        W = []
        W = (SS*numpy.sqrt(T))/I # Computes contribution of the sorptivity component
        if numpy.max(W) >=  1 - d and numpy.max(W) <= 1 + d: # Checks the selection index of the procedure
            t_char = tc
            I_char = Ic
            aa = (1/(9*(1-omega)))*(beta**2 - beta + 1) * (t_char**2)/(I_char)
```

(Continues)

```python
        bb = ((2 - beta) / 3) * t_char
        cc = -1 * omega * I_char
        Kp = (numpy.sqrt(bb**2 - 4 * aa * cc) - bb) / (2 * aa) # Computes the Ks
        Sp = (1-omega)*(I_char/numpy.sqrt(t_char))
        break
    return t_char, I_char, Sp, Kp
def CTM_Ks(Sp, t_char, I_char, omega, beta, T, I):
    W = Sp*numpy.sqrt(T)/I
    del W[0]
    del T[0]
    ## Use linregress if you do not want to set the intercept to zero: ln(W) = a + bT
    Stat = scipy.stats.linregress(T, numpy.log(W))
    alpha = Stat.slope
    ## Use lin_fit if you want to set the intercept to zero: ln(W) = bT
    #alpha = lin_fit(T, numpy.log(W))
    #alpha = float(alpha)
    if omega = = 0.5:
        t_grav = t_char
        I_grav = I_char
    else:
        t_grav = numpy.log(0.5)/alpha
        I_grav = (Sp*numpy.sqrt(t_grav))/0.5
    # Calculate Ks
    a1 = (2*(beta**2 - beta +1)* t_grav**2)/(9*I_grav)
    b1 = ((2-beta)/3)*t_grav
    c1 = -1*0.5*I_grav
    Kp = (numpy.sqrt(b1**2 - 4*a1*c1)-b1)/(2*a1)
    return Kp, t_grav, I_grav, alpha
def lin_fit(x, y):
    #'''Fits a linear fit of the form mx+b to the data'''
    fitfunc = lambda params, x: params[0] * x    #create fitting function of form mx
    errfunc = lambda p, x, y: fitfunc(p, x) - y       #create error function for least squares fit
    init_a = -1           #find initial value for a (gradient)
    init_p = numpy.array((init_a))    #bundle initial values in initial parameters
    #calculate best fitting parameters (i.e. m and b) using the error function
    p1, success = scipy.optimize.leastsq(errfunc, init_p.copy(), args = (x, y))
    #f = fitfunc(p1, x)   #create a fit with those parameters
    return p1
# Predicting S and Ks
Sp, Kp1, Kp2, t_char, I_char, t_grav, I_grav, omega, alpha = CTM(T, I, beta)
# Printing the results
```

```
print('—————————————-')
print ('————-> Results <————-')
print('—————————————-')
print('Predicted S =', round(Sp, 2), '[L/sqrt(T)]')
print('Predicted Ks by CTM-Ks', round(Kp2,2), '[L/T]')
print('Predicted Ks by CTM-I', round(Kp1,2), '[L/T]')
print('t_char =', round(t_char,2), '[T]')
print('I_char =', round(I_char,2), '[L],')
print('t_grav =', round(t_grav,2), '[T]')
print('I_grav =', round(I_grav,2), '[L],')
print('omega =', round(omega,2), '[-]')
print('alpha =', round(alpha,4), '[1/T]')
```